DOI: 10.1002/ejic.200601030

Solvothermal Synthesis, Crystal Structure, and Thermal Stability of Three-Layered Thioantimonate(III) Complexes: $[Ni(C_3H_{10}N_2)_3]Sb_4S_7$, $[C_4H_{14}N_2]Sb_8S_{13}\cdot H_2O$, and $[C_6H_{18}N_2]Sb_{10}S_{16}\cdot H_2O$

Meng Zhang,[a,b] Tian Lu Sheng,[a] Xi He Huang,[a] Rui Biao Fu,[a] Xin Wang,[a] Sheng Min Hu,[a] Sheng Chang Xiang,[a] and Xin Tao Wu*[a]

Keywords: Thioantimonates / Solvothermal synthesis / Cations / Layered compounds

Three new thioantimonate(III) complexes $[Ni(1,2\text{-PDA})_3]Sb_4S_7$ (**1**) (1,2-PDA = 1,2-propanediamine), $[dmenH_2^{2+}]Sb_8S_{13}\cdot H_2O$ (**2**) (dmen = *N*,*N*-dimethylethylenediamine), and $[deenH_2^{2+}]Sb_{10}S_{16}\cdot H_2O$ (**3**) (deen = *N*,*N*-diethylethylenediamine), prepared under solvothermal conditions, have been characterized by single-crystal X-ray diffraction, elemental analysis, and DTA-TG measurements. In compound **1**, a rectangle-like $Sb_{16}S_{16}$ heterоring whose dimensions are about 8.1×14.7 Å is observed, this is the largest reported pore in layered thioantimonates to date. Further condensation of the $Sb_{16}S_{16}$ heterorings resulted in an unprecedented framework of the five-atom thick $Sb_xS_y^{n-}$ layer. In **2**, a new member of Sb_nS_n (n = 2, 3, 4, 8, 16, 30, 31, 32) heterocycles $Sb_{15}S_{15}$ heterоring has been obtained as the first example. In compound **3**, the most particular feature is that when the secondary Sb–S bonds are considered the Sb2 atom becomes sevenfold coordinated.

Introduction

The design and synthesis of chalcogenidometalates have received considerable attention[1–3] during the past decades. To design and synthesize more compounds with various configurations, it is very important to understand which factors affect the structures of chalcogenidometalates. We have in some extent studied how the structures of the sulfur-containing transition-metal polymers are influenced by the size and charge of the cations.[1,2] By using different cations such as $[Nd(DMF)_8]^{3+}$ and $[La(DMF)_8]^{3+}$, we have successfully synthesized and characterized a large number of complexes with different structure.[4] Now we further spread our interest to the study of thioantimonates.

Dozens of open-framework thioantimonates, in which transition-metal complex cations[5–18,25] and organic amine cations[19–24] serve as charge balancing ions, have been prepared in recent years, and the synthesis of these compounds is generally completed in the presence of organic amines as structure-directing agents.[10,20,26,27,34] The organic species used are often aliphatic amines, polyamines, and alicyclic amines.[21–32] The solvothermal method was proven to be very successful in the synthesis of these compounds. Although the size and charge of cations obviously have important effects on the final structure of the anions,[17,19,23,27,32] a clear relationship between them has not been observed.[12,13] Therefore, more examples of such compounds need to be prepared for further understanding.

In this work, $[Ni(1,2\text{-PDA})_3]Sb_4S_7$ (**1**) is the first example of a thioantimonate(III) in which a 1,2-propanediamine complex of a transition metal serves as the counterion. As a result of the use of two N-substituted polyamines, *N*,*N*-dimethylethylenediamine and *N*,*N*-diethylethylenediamine, we successfully prepared two additional thioantimonate(III) complexes: $[C_4H_{14}N_2]Sb_8S_{13}\cdot H_2O$ (**2**) and $[C_6H_{18}N_2]Sb_{10}S_{16}\cdot H_2O$ (**3**).

Results and Discussion

The structure of compound **1** is composed of isolated $[Ni(1,2\text{-PDA})_3]^{2+}$ cations and $^2_\infty[Sb_4S_7]^{2-}$ anions. The Ni^{2+} ion is sixfold coordinated by six nitrogen atoms of bichelate 1,2-PDA ligands, which forms a distorted octahedron (Figure 1), as is suggested by the octahedral axial $N\text{–}Ni\text{–}N_{trans}$ angles between 171.6(4)° and 172.4(4)°. The Ni–N distances between 2.091(9) and 2.135(9) Å (Table 1) are comparable with those reported in the literature.[33,34] The $^2_\infty[Sb_4S_7]^{2-}$ anion consists of two SbS_3 trigonal pyramids and two SbS_4 units. The Sb–S distances in SbS_3 pyramids vary from 2.373(3) to 2.561(2) Å with S–Sb–S angles between 90.89(7)° and 98.19(9)° (Table 1). For SbS_4 units, both Sb

[a] State Key Laboratory of Structural Chemistry, Fujian Institute of Research on the Structure of Matter, The Chinese Academy of Sciences,
Fuzhou, Fujian 350002, China
Fax: +86-591-83714947
E-mail: wxt@fjirsm.ac.cn
[b] Graduate University of the Chinese Academy of Sciences, Beijing 100039, China

Supporting information for this article is available on the WWW under http://www.eurjic.org or from the author.

atoms have two short and two longer distances to neighboring S atoms with longer Sb–S separations in the *trans* position, the Sb–S bond lengths and S–Sb–S angles range, respectively, from 2.429(2) to 2.744(3) Å and from 81.29(8)° to 169.84(8)° (Table 1). These values are normal and comparable to other thioantimonate(III) complexes.[13,35,36] The interconnection of primary building units (PBUs) $Sb1S_4$, $Sb2S_3$, $Sb3S_3$, and $Sb4S_4$ results in an Sb_4S_{10} chain (Figure 2). Through sharing S1 and S2 atoms, four chains of this condense to an $Sb_{16}S_{16}$ ring whose dimensions are about 8.1×14.7 Å (measured from coordinate to coordinate); this is the largest pore in layered thioantiomonates by far.[10,12,13,20] Further condensation of $Sb_{16}S_{16}$ rings through common S7 and S7b atoms leads to the two-dimensional layered $[Sb_4S_7]^{2-}$ anion, which is the first "five-atom"-thick layer; an overwhelming number of thioantimonate(III) complexes that have two-atom-thick layers are often found.[12] The layers lie in the (100) plane, and they are stacked onto each other along the *a* axis to form tunnels also in this direction (Figure 3). The cations are located between the layers.

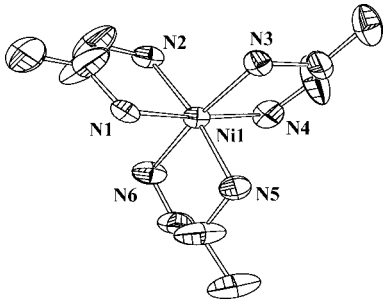

Figure 1. Structure of $[Ni(1,2\text{-}PDA)_3]^{2+}$ cation in **1** with labeling. Hydrogen atoms are omitted for clarity, displacement ellipsoids are drawn at the 50% probability level.

Table 1. Selected distances [Å] and angles [°] for $[Ni(C_3H_{10}N_2)_3]Sb_4S_7$ (**1**).[a]

Sb1–S1	2.368(2)	Sb4–S2a	2.429(2)
Sb1–S4	2.459(3)	Sb4–S7	2.469(2)
Sb1–S2	2.680(3)	Sb4–S6	2.700(2)
Sb1–S3	2.842(3)	Sb4–S1a	2.744(3)
Sb2–S3	2.373(3)	Ni1–N2	2.091(9)
Sb2–S5	2.447(3)	Ni1–N1	2.112(8)
Sb2–S4	2.489(3)	Ni1–N5	2.125(8)
Sb3–S6	2.422(2)	Ni1–N6	2.130(9)
Sb3–S7b	2.470(2)	Ni1–N4	2.130(9)
Sb3–S5	2.561(2)	Ni1–N3	2.135(9)
S1–Sb1–S4	103.25(9)	S6–Sb3–S7b	97.64(8)
S1–Sb1–S2	86.32(8)	S6–Sb3–S5	92.72(8)
S4–Sb1–S2	90.27(9)	S7b–Sb3–S5	87.82(8)
S1–Sb1–S3	90.11(8)	S2a–Sb4–S7	104.05(9)
S4–Sb1–S3	81.29(8)	S2a–Sb4–S6	89.14(8)
S2–Sb1–S3	169.84(8)	S7–Sb4–S6	89.97(8)
S3–Sb2–S5	98.19(9)	S2a–Sb4–S1a	83.73(8)
S3–Sb2–S4	90.87(9)	S7–Sb4–S1a	83.73(8)
S5–Sb2–S4	98.08(9)	S6–Sb4–S1a	169.04(8)

[a] Symmetry codes: a: $-x+5/2$, $y+1/2$, $-z+1/2$, b: $-x+3$, $-y+2$, $-z+1$.

The structure of compound **2** consists of double-protonated dmen cations and $^2_\infty[Sb_8S_{13}]^{2-}$ anions, seven SbS_3 trigonal pyramids, and one SbS_4 unit as the PBUs condense to form the $[Sb_8S_{13}]^{2-}$ anion through sharing common corners and edges (Figure 4). The Sb–S separations of the SbS_3 pyramids vary from 2.396(2) to 2.567(2) Å with the S–Sb–S angles between 85.69(4)° and 98.23(4)°. In the $Sb6S_4$ unit, the Sb6 atom has two short [2.447(2) and 2.532(2) Å] and two relatively longer distances [2.747(2) and 2.728(2) Å], the longer distances being in the *trans* position [170.00(4)°]

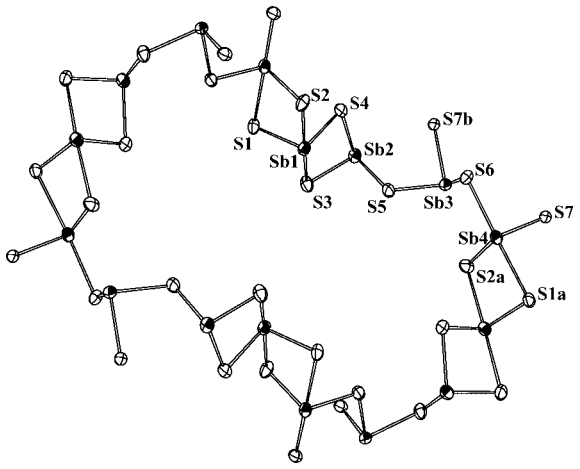

Figure 2. Sb_4S_{10} chain with labeling and further condensation to form $Sb_{16}S_{16}$ ring in $[Ni(C_3H_{10}N_2)_3]Sb_4S_7$ (**1**). Symmetry codes: a: $-x+5/2$, $y+1/2$, $-z+1/2$, b: $-x+3$, $-y+2$, $-z+1$. Displacement ellipsoids are drawn at the 50% probability level.

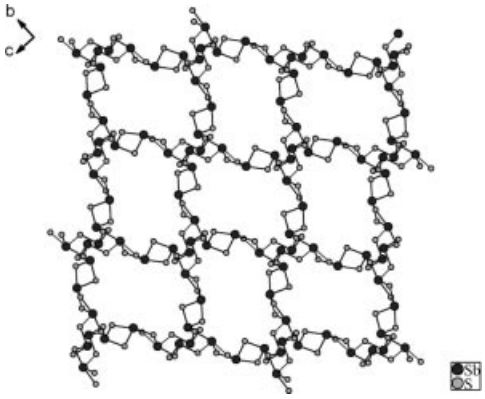

Figure 3. The layer composed of $Sb_{16}S_{16}$ rings in $[Ni(C_3H_{10}N_2)_3]Sb_4S_7$ (**1**).

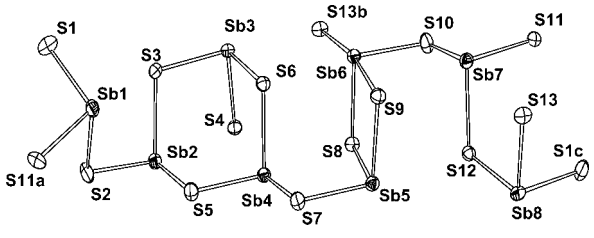

Figure 4. Condensation of seven SbS_3 trigonal pyramids and one SbS_4 unit to form the $[Sb_8S_{13}]^{2-}$ anion with numbering scheme in $[C_4H_{14}N_2]Sb_8S_{13}\cdot H_2O$ (**2**). Symmetry codes: a: –x, $-1/2+y$, $1/2-z$, b: $-1+x$, y, z, c: $-x$, $1/2+y$, $1/2-z$. Displacement ellipsoids are drawn at the 50% probability level.

(Table 2). All these values are normal in thioantimonate(III) complexes.[19,22,23] Further interconnection of the $[Sb_8S_{13}]^{2-}$ anions yields undulated layers extending in the (001) plane, in which the $Sb_{15}S_{15}$ heterorings are for the first time observed (shadowed area in Figure 5). There exist nearly circular pores with dimensions of about 7.9×8.4 Å (measured from coordinate to coordinate) in these heterorings. The layers are stacked onto each other to build channels along the *c* axis, in which the organic cations and the water molecules are accommodated (Figure 5). Compound **3** is composed of double-protonated deen cations and $^2_\infty[Sb_{10}S_{16}]^{2-}$ anions. The $[Sb_{10}S_{16}]^{2-}$ anions are formed by the interconnection of nine SbS_3 trigonal pyramids and one SbS_4 unit by common corners and edges (Figure 6). In the SbS_3 pyramids, Sb–S distances vary from 2.404(3) to 2.595(3) Å and S–Sb–S angles are between 87.58(10)° and 98.70(10)°; in the $Sb6S_4$ moieties there are three short [2.460(3), 2.506(3), Sb6–S9: 2.585(3) Å] and one extraordinarily long Sb–S bonds [Sb6–S15a: 2.929(3) Å] with the S9–Sb6–S15a angle being 169.61(10)° (Table 3). All of these values are in the typical range.[21,22,27] Further condensation of the $[Sb_{10}S_{16}]^{2-}$ anions resulted in the two-dimensional layers extending in the (001) plane, which could be thought

Table 2. Selected distances [Å] and angles [°] for $[C_4H_{14}N_2]$-$Sb_8S_{13}\cdot H_2O$ (**2**).[a]

Sb1–S11a	2.437(2)	S11a–Sb1–S1	100.59(5)
Sb1–S2	2.440(2)	S2–Sb1–S1	93.48(5)
Sb1–S1	2.452(2)	S3–Sb2–S5	97.22(4)
Sb2–S3	2.445(2)	S3–Sb2–S2	90.89(4)
Sb2–S5	2.451 (2)	S5–Sb2–S2	88.88(5)
Sb2–S2	2.496(2)	S4–Sb3–S6	92.99(4)
Sb3–S4	2.396 (2)	S4–Sb3–S3	92.43(4)
Sb3–S6	2.507(2)	S6–Sb3–S3	96.60(4)
Sb3–S3	2.513 (2)	S6–Sb4–S5	93.30(4)
Sb4–S6	2.465(2)	S6–Sb4–S7	90.12(4)
Sb4–S5	2.498(2)	S5–Sb4–S7	92.93(4)
Sb4–S7	2.533(2)	S9–Sb5–S7	94.62(4)
Sb5–S9	2.417(2)	S9–Sb5–S8	89.98(4)
Sb5–S7	2.535(2)	S7–Sb5–S8	98.23(4)
Sb5–S8	2.567(2)	S8–Sb6–S10	93.34(5)
Sb6–S8	2.447(2)	S8–Sb6–S9	85.69(4)
Sb6–S10	2.532(2)	S10–Sb6–S9	93.96(4)
Sb6–S9	2.728(2)	S8–Sb6–S13b	88.99(4)
Sb6–S13b	2.747(2)	S10–Sb6–S13b	94.80(4)
Sb7–S10	2.461(2)	S9–Sb6–S13b	170.00(4)
Sb7–S12	2.475(2)	S10–Sb7–S12	89.89(4)
Sb7–S11	2.497(2)	S10–Sb7–S11	93.07(5)
Sb8–S13	2.413(2)	S12–Sb7–S11	94.81(4)
Sb8–S12	2.477(2)	S13–Sb8–S12	96.50(4)
Sb8–S1c	2.524(2)	S13–Sb8–S1c	96.17(5)
S11a–Sb1–S2	86.82(5)	S12–Sb8–S1c	91.96(4)

[a] Symmetry codes: a: -x, y–1/2, –*z*+1/2, b: x–1, *y*, *z*, c: –x, *y*+1/2, –*z*+1/2.

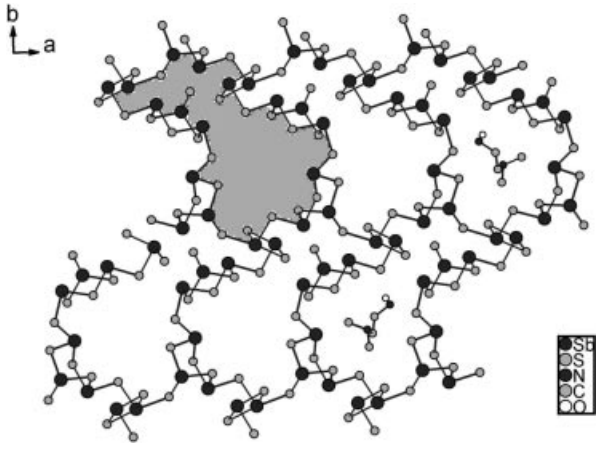

Figure 5. $Sb_{15}S_{15}$ heteroring (shadowed area) in layer of $[C_4H_{14}N_2]$-$Sb_8S_{13}\cdot H_2O$ (**2**). The organic cations and water molecules are accommodated in the channels. Hydrogen atoms, some organic cations, and H_2O molecules are omitted for clarity.

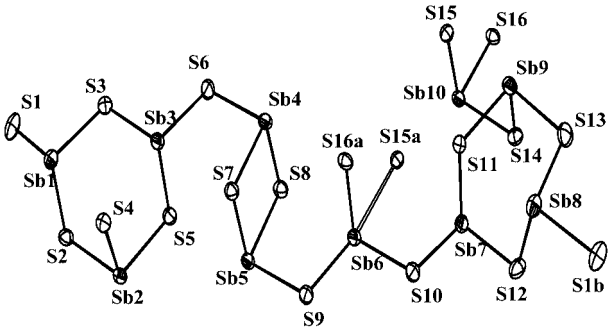

Figure 6. Interconnection of nine SbS_3 and one SbS_4 units, which results in the $[Sb_{10}S_{16}]^{2-}$ anion with labeling in $[C_6H_{18}N_2]$-$Sb_{10}S_{16}\cdot H_2O$ (**3**). Symmetry codes: a: 2 –*x*, -y, 2 –*z*, b: 1 –*x*, –1/2 + *y*, 3/2 –*z*.

Table 3. Selected distances [Å] and angles [°] for $[C_6H_{18}N_2]$-$Sb_{10}S_{16}\cdot H_2O$ (**3**).[a]

Sb1–S2	2.443(3)	S2–Sb1–S1	89.70(11)
Sb1–S3	2.469(3)	S3–Sb1–S1	89.75(12)
Sb1–S1	2.498(3)	S4–Sb2–S5	96.04(10)
Sb2–S4	2.404(3)	S4–Sb2–S2	91.50(11)
Sb2–S5	2.468(3)	S5–Sb2–S2	96.88(10)
Sb2–S2	2.521(3)	S5–Sb3–S3	94.97(11)
Sb3–S5	2.453(3)	S5–Sb3–S6	90.46(11)
Sb3–S3	2.492(3)	S3–Sb3–S6	93.73(11)
Sb3–S6	2.515(3)	S8–Sb4–S7	89.30(10)
Sb4–S8	2.449(3)	S8–Sb4–S6	94.84(11)
Sb4–S7	2.519(3)	S7–Sb4–S6	97.61(10)
Sb4–S6	2.521(3)	S7–Sb5–S9	93.36(10)
Sb5–S7	2.480(3)	S7–Sb5–S8	87.58(10)
Sb5–S9	2.521(3)	S9–Sb5–S8	98.70(10)
Sb5–S8	2.564(3)	S16a–Sb6–S10	93.16(11)
Sb6–S16a	2.460(3)	S16a–Sb6–S9	90.40(10)
Sb6–S10	2.506(3)	S10–Sb6–S9	93.66(10)
Sb6–S9	2.585(3)	S16a–Sb6–S15a	81.83(9)
Sb6–S15a	2.929(3)	S10–Sb6–S15a	93.65(9)
Sb7–S10	2.461(3)	S9–Sb6–S15a	169.61(10)
Sb7–S11	2.495(3)	S10–Sb7–S11	91.73(10)
Sb7–S12	2.498(3)	S10–Sb7–S12	92.73(12)
Sb8–S12	2.438(3)	S11–Sb7–S12	95.03(10)
Sb8–S1b	2.444(4)	S12–Sb8–S1b	88.40(12)
Sb8–S13	2.459(4)	S12–Sb8–S13	98.68(13)
Sb9–S14	2.457(3)	S1b–Sb8–S13	92.68(13)
Sb9–S11	2.478(3)	S14–Sb9–S11	96.13(10)
Sb9–S13	2.509(3)	S14–Sb9–S13	93.58(12)
Sb10–S15	2.422(3)	S11–Sb9–S13	92.78(11)
Sb10–S16	2.519(3)	S15-Sb10–S16	91.75(10)
Sb10–S14	2.595(3)	S15-Sb10–S14	92.37(10)
S2–Sb1–S3	97.59(11)	S16-Sb10–S14	98.31(10)

[a] Symmetry codes: a: 2–*x*, –y, 2–*z*, b: 1–*x*, –1/2+*y*, 3/2–*z*.

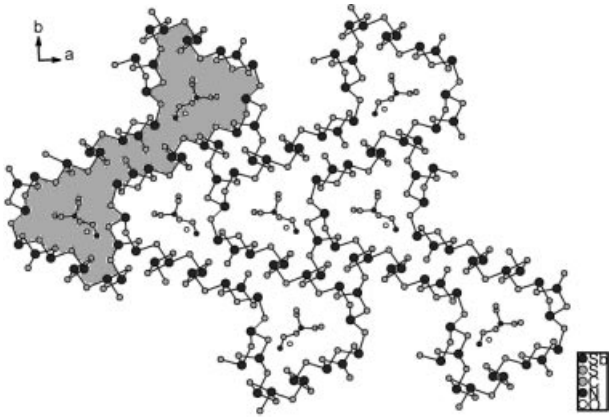

Figure 7. $[Sb_{10}S_{16}]^{2-}$ layer consists of $Sb_{30}S_{30}$ rings (shaded area) in $[C_6H_{18}N_2]Sb_{10}S_{16}\cdot H_2O$ (**3**). Organic cations and water molecules are held in tunnels. Hydrogen atoms are omitted for clarity.

to be composed of the "double-ellipsoidal"[20] $Sb_{30}S_{30}$ rings in two perpendicular directions (Figure 7). The dimensions of the ellipsoidal pores in the $Sb_{30}S_{30}$ rings are about 8.8×10.1 Å (measured from coordinate to coordinate). The layers are stacked onto each other in the [001] direction, which forms channels where the cations and water molecules are located (Figure 7).

In all three title compounds, relatively short H···S distances are observed. The short H···S separations in compound $[Ni(C_3H_{10}N_2)_3]Sb_4S_7$ scatter from 2.51 to 2.69 Å with N–H···S angles ranging from 157.5° to 177.9° (Table 4). In $[C_4H_{14}N_2]Sb_8S_{13}\cdot H_2O$, four short H···S contacts from 2.53 to 2.82 Å are found with N–H···S (or O–H···S) angles between 136.1° and 163.8° (Table 4). Several short H···S separations (2.46 to 2.60 Å) in $[C_6H_{18}N_2]$-$Sb_{10}S_{16}\cdot H_2O$ are also observed, and the N–H···S (or O–H···S) angles are in the range of 140.6 to 164.2° (Table 4). All the values indicate that weak hydrogen bonding interconnections exist between the cations and the $Sb_xS_y^{n-}$ anions.

When the secondary Sb–S bonds (sum of van der Waals' radii: $Sb_{vdw} + S_{vdw} \approx 3.85$ Å[37]) are taken into account, most Sb atoms in the three title compounds enhance their coordination numbers. In compound **1**, the Sb3 and Sb4 atoms are fivefold coordinated to form ψ-SbS_5 octahedra, and the Sb2 atom is surrounded by four S atoms to yield ψ-SbS4 trigonal bipyramids (Table 5). In compound **2**, the Sb1 and Sb7 atoms enhance their coordination numbers to five and the Sb2, Sb3, Sb4, Sb5, Sb6, and Sb8 atoms become sixfold coordinated (Table 5). In compound **3**, the Sb1 atom, the Sb7 and Sb8 atoms, and the Sb3, Sb4, Sb5, Sb6, Sb9, and Sb10 atoms are surrounded by four, five, and six S atoms, respectively. The most distinct character is that the Sb2 atom becomes seven-coordinate (Figure 8) with the Sb–S bond lengths varying from 3.1909(31) to 3.7607(34) Å and the S–Sb–S angles being in the range of 59.91(8)° to111.29(8)° [67.98(7) to113.14(6)° for other Sb atoms] (Table 5). To the best of our knowledge, compound **3** is the first thioantimonate in which there exists seven-coordinate Sb atoms with Sb–S distances under 3.8 Å.

In the three title compounds, the sequence of the cationic size is $[Ni(C_3H_{10}N_2)_3]^{2+}$ (in **1**) > $[C_6H_{18}N_2]^{2+}\cdot H_2O$ (in **3**) > $[C_4H_{14}N_2]^{2+}\cdot H_2O$ (in **2**), correspondingly the dimensions of pores in compounds are **1** (8.1×14.7 Å) > **3** (8.8×10.1 Å) > **2** (7.9×8.4 Å), the cations and the water molecules are

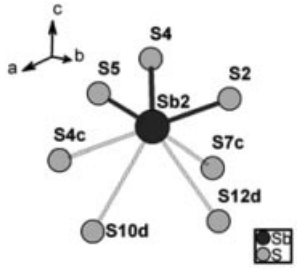

Figure 8. Seven-coordinated Sb2 atom in $[C_6H_{18}N_2]Sb_{10}S_{16}\cdot H_2O$ (**3**). Symmetry code: c: –x, -y, 1 –*z*, d: 1 –*x*, -y, 1 –*z*.

Table 4. Proposed hydrogen bonding geometry for $[Ni(C_3H_{10}N_2)_3]Sb_4S_7$ (**1**), $[C_4H_{14}N_2]Sb_8S_{13}\cdot H_2O$ (**2**), and $[C_6H_{18}N_2]Sb_{10}S_{16}\cdot H_2O$ (**3**).

D–H	A	*d*(H···A)	*d*(D···A)	<DHA	Symmetry code
$[Ni(C_3H_{10}N_2)_3]Sb_4S_7$					
N1–H1A	S1	2.55	3.396(8)	157.5	
N1–H1B	S5	2.69	3.570(9)	164.6	x-1, *y*, *z*
N2–H3A	S4	2.63	3.526(9)	177.9	–*x* + 3/2, y-1/2, –*z* + 1/2
N2–H3B	S6	2.57	3.451(9)	165.4	–*x* + 3/2, y-1/2, –*z* + 1/2
N3–H2B	S5	2.51	3.365(9)	159.3	x-1, *y*, *z*
$[C_4H_{14}N_2]Sb_8S_{13}\cdot H_2O$					
N2–H2A	S7	2.54	3.404(6)	163.8	–x-1, –*y* + 1, –*z* + 1
N2–H2C	S1	2.82	3.516(6)	136.1	
O1–H1D	S10	2.58	3.265(5)	138.3	
O1–H1E	S1	2.53	3.302(5)	152.0	x-1, *y*, *z*
$[C_6H_{18}N_2]Sb_{10}S_{16}\cdot H_2O$					
N1–H1C	S2	2.60	3.338(11)	140.6	x + 1, *y*, *z*
N1–H1D	S9	2.59	3.367(13)	146.9	–x, *y* + 1/2, –*z* + 3/2
O1–H1F	S6	2.46	3.284(11)	164.2	x + 1, *y*, *z*

Table 5. The long Sb–S bonds [Å] and some S–Sb–S angles [°] in compounds **1**–**3**.[a]

$[Ni(C_3H_{10}N_2)_3]Sb_4S_7$ (**1**)			
Sb2–S7b	3.6197(24)	Sb3–S2a	3.4969(25)
Sb3–S6b	3.0593(25)	Sb4–S3c	3.5010(26)
$[C_4H_{14}N_2]Sb_8S_{13}{\cdot}H_2O$ (**2**)			
Sb1–S12a	3.2707(13)	Sb5–S4f	3.0826(13)
Sb1–S3	3.3016(13)	Sb5–S12	3.2860(13)
Sb2–S4	3.1035(13)	Sb5–S7h	3.5613(14)
Sb2–S7b	3.7021(13)	Sb6–S6	3.1086(13)
Sb2–S4g	3.7351(13)	Sb6–S13j	3.6998(14)
Sb3–S9b	3.2233(13)	Sb7–S9	3.1479(14)
Sb3–S13b	3.3178(15)	Sb7–S13	3.2971(13)
Sb3–S11i	3.4816(13)	Sb8–S4f	3.2472(13)
Sb4–S4	3.0214(13)	Sb8–S8f	3.3889(12)
Sb4–S8	3.1146(13)	Sb8–S2h	3.7584(15)
Sb4–S4g	3.6241(13)		
$[C_6H_{18}N_2]Sb_{10}S_{16}{\cdot}H_2O$ (**3**)			
Sb1–S4	3.0925(31)	Sb7–S15a	3.1317(31)
Sb3–S4	3.0495(31)	Sb7–S14	3.3374(31)
Sb3–S7	3.1997(31)	Sb8–S2b	3.2598(31)
Sb4–S16a	3.1594(33)	Sb8–S11	3.2789(30)
Sb4–S14a	3.1863(31)	Sb9–S15	3.0792(31)
Sb4–S14j	3.5548(33)	Sb9–S8a	3.5946(30)
Sb5–S4c	3.0754(31)	Sb9–S3i	3.6282(34)
Sb5–S5	3.2465(32)	Sb10-S15a	3.1056(30)
Sb5–S9d	3.3800(34)	Sb10-S11a	3.1312(30)
Sb6–S8	3.1415(33)	Sb10-S6h	3.4291(37)
Sb6–S4h	3.5750(32)		
Sb2–S4c	3.1909(31)	Sb2–S12d	3.4002(33)
Sb2–S7c	3.3842(30)	Sb2–S10d	3.7607(34)
S7c–Sb2–S4c	85.05(8)	S10d–Sb2–S4c	67.30(7)
S12d–Sb2–S4c	111.29(8)	S10d–Sb2–S7c	107.10(7)
S12d–Sb2–S7c	72.57(8)	S10d–Sb2–S12d	59.91(8)

[a] Symmetry codes: for $[Ni(C_3H_{10}N_2)_3]Sb_4S_7$: a: $-x+5/2$, $y+1/2$, $-z+1/2$, b: $-x+3$, $-y+2$, $-z+1$, c: $x+1$, y, z; for $[C_4H_{14}N_2]Sb_8S_{13}{\cdot}H_2O$: a: –x, y–1/2, $-z+1/2$, b: x–1, y, z, f: $x+1$, y, z, g: –x–1, $-y+1$, –z, h: -x, $-y+1$, –z, i: -x, $-y+1$, $-z+1$, j: $-x+1$, $-y+1$, $-z+1$; for $[C_6H_{18}N_2]Sb_{10}S_{16}{\cdot}H_2O$: a: $-x+2$, $-y$, $-z+2$, b: $-x+1$, y–1/2, $-z+3/2$, c: –x, $-y$, $-z+1$, d: $-x+1$, $-y$, $-z+1$, h: $x+1$, y, z, i: $-x+1$, $-y$, $-z+2$, j: x–1, y, z.

located above or under the pores. So it is obvious that the cations play an important role in the formation of $Sb_xS_y^{n-}$ structures.

Thermal Investigations

Compound **1** decomposes in a two-step manner which is accompanied by two signals in the DTA curve (T_p = 192 and 286 °C; Figure S1) and the extrapolated onset temperature T_e was 175 °C. The experimental total mass loss was 24.4%, which corresponds to the emission of organic amine ($-\Delta m_{theo}$ = 22.4%). For **2**, the mechanism of decomposition is more complicated and two obvious steps can be identified. In the first step, the extrapolated onset temperature T_e was 140 °C and T_p was 150 °C (Figure S2). The weight loss was 1.2%, which is in good agreement with the expected value for the removal of water molecules ($-\Delta m_{theo}$ = 1.0%). On further heating, another endothermic event occurred with the DTA signal at T_p = 274 °C, the mass loss was 8.4% which can be attributed to the complete emission of organic ligands ($-\Delta m_{theo}$ = 6.0%). In the TG curve of **3** a smooth decrease from 63 °C to 223 °C is observed with a weight change of 1.1% (Figure S3), as corresponds to the removal of water molecules ($-\Delta m_{theo}$ = 1.0%). On further heating, a sharp weight loss of 7.6% occurred, which was accompanied by the endothermic event at T_e = 247 °C and T_p = 260 °C in the DTA curve. The experimental value is in good agreement with that determined for the emission of the organic component ($-\Delta m_{theo}$ = 6.3%). During the heating process, besides the removal of organic amine and water molecules, some H_2S molecules were formed and emitted.[13,27] This may explain the discrepancy between the experimental and theoretic values.

Experimental Section

1: Yellow crystals of $[Ni(1,2\text{-PDA})_3]Sb_4S_7$ (**1**) were obtained from Ni (0.0586 g, 1 mmol) or $NiCl_2{\cdot}6H_2O$ (0.273 g, 1 mmol), Sb (0.1217 g, 1 mmol), and S (0.1280 g, 4 mmol) in a water solution of 1,2-PDA (60%, 5 mL) under solvothermal conditions. The mixture was heated at 140 °C for 6 d in Teflon-lined steel autoclaves with an inner volume of 25 mL and then cooled to room temperature over 5 h. After the reaction mixture was filtered, the residual solid product was washed with alcohol. The yellow crystals were obtained in 30% yield (according to Sb), and they are stable in air and alcohol, but have good dissolvability in water. $C_9H_{30}N_6NiSb_4S_7$ (992.52): calcd. C 10.8, H 3.02, N 8.46; found C 10.54, H 3.23, N 8.95.

2: Red crystals of $[dmenH_2^{2+}]Sb_8S_{13}{\cdot}H_2O$ (**2**) were prepared from the reaction of Zn (0.0915 g, 1.4 mmol), Sb (0.1217 g, 1 mmol), and S (0.1280 g, 4 mmol) in an aqueous solution of dmen (50%, 5 mL). The mixture was heated at 140 °C for 6 d in Teflon-lined steel autoclaves and then cooled to room temperature. The reacted mixture was filtered and washed with water and alcohol to give 30% yield of crystalline **2** (based on Sb). The product is stable in air, water, and ethanol. In the absence of Zn in the reaction mixture, a decreased yield was observed. $C_4H_{16}N_2Sb_8S_{13}O$ (1498.97): calcd. C 3.20, H 1.06, N 1.87; found C 3.55, H 1.36, N 1.67.

3: The procedure for the synthesis of $[deenH_2^{2+}]Sb_{10}S_{16}{\cdot}H_2O$ (**3**) is the same as that of **2**. Zn (0.0729 g, 1.1 mmol), Sb (0.1217 g, 1 mmol), S (0.0712 g, 2.2 mmol), aqueous solution of deen (50%, 5 mL). Yield: 35%. In the absence of Zn in the reaction mixture, a decreased yield was observed. $C_6H_{20}N_2Sb_{10}S_{16}O$ (1866.70): calcd. C 3.86, H 1.07, N 1.50; found C 3.82, H 1.35, N 1.23.

Structure Determination: Intensities were collected at 293(2) K with a Simens SMART-CCD diffractometer (for **1**), at 294(2) K with a Rigaku SATURN70 CCD diffractometer (for **2**), and at 293(2) K with a Rigaku Mercury CCD diffractometer (for **3**) by using graphite-monochromated Mo-K_a radiation [λ = 0.71073 Å]. Data for all three compounds were corrected for Lorentz, polarization, and absorption effects. The structures were solved and refined by full-matrix least-squares techniques on F^2 by using SHELXL-97,[38] all non-hydrogen atoms were refined anisotropically. Hydrogen atoms were generated geometrically and allowed to ride on their parent atoms with fixed isotropic displacement parameters. The crystallographic data are summarized in Table 6.

CCDC-626004 (for **1**), -626005 (for **2**), and -626006 (for **3**) contain the supplementary crystallographic data for this paper. These data

Table 6. Crystallographic data for $[Ni(C_3H_{10}N_2)_3]Sb_4S_7$ (**1**), $[C_4H_{14}N_2]Sb_8S_{13}\cdot H_2O$ (**2**), and $[C_6H_{18}N_2]Sb_{10}S_{16}\cdot H_2O$ (**3**).

	1	**2**	**3**
Color, habit	yellow block	red sheet	red block
Crystal size [mm]	$0.25\times0.25\times0.20$	$0.18\times0.12\times0.01$	$0.24\times0.22\times0.20$
Crystal system	monoclinic	monoclinic	monoclinic
Space group	*P*21/*n*	*P*21/*c*	*P*21/*c*
a [Å]	10.809(1)	9.143(2)	11.537(3)
b [Å]	15.795(1)	23.515(4)	25.110(7)
c [Å]	16.1152(2)	13.871(2)	13.748(4)
β [°]	90.75(1)	105.00(1)	111.29(1)
V [Å^3]	2751.11(5)	2880.6(8)	3711.0(18)
Z	4	4	4
Formula weight [g mol^{-1}]	992.52	1498.97	1866.70
Calculated density [g cm^{-3}]	2.396	3.456	3.341
μ [mm^{-1}]	5.091	8.332	8.070
F(000)	1880	2712	3376
Temperature [K]	293(2)	293(2)	293(2)
θ range for data collection [°]	1.81 to 25.66	2.30 to 27.47	2.27 to 27.48
h, *k*, *l*, range	–13 to 8	–11 to 11	–14 to 11
	–19 to19	–30 to 23	–30 to 32
	–19 to 16	–18 to 18	–15 to 17
Reflections measured	14489	22025	28691
Independent reflections	5201	6496	8491
Observed reflection [$I>2\sigma(I)$]	4488	5725	7281
$R_{int.}$	0.0363	0.0322	0.0639
Min./max. trans.	0.8146/1.0000	0.6135/1.0000	0.2476/0.2952
R[a]	0.0446	0.0213	0.0622
Rw[b]	0.0890	0.0552	0.1516
Goodness of fit	1.096	1.199	1.177
Max./min. $\Delta\rho$ [e Å^{-3}]	1.286/–0.954	1.242/–1.187	1.861/–1.954

[a] $R = \Sigma(||F_o| - |F_c||)/\Sigma|F_o|$. [b] $Rw = \{\Sigma w[(F_o^2 - F_c^2)^2]/\Sigma w[(F_o^2)^2]\}^{1/2}$, $w = 1/[\sigma^2(F_o^2)+(aP)^2+bP]$, $P = (F_o^2+2F_c^2)/3$, $a = 0.1110$, $b = 14.4871$.

can be obtained free of charge from The Cambridge Crystallographic Data Centre via www.ccdc.cam.ac.uk/data_request/cif.

Thermoanalytical Measurements: Thermoanalytical measurements were performed with a DTA-TG device STA 449C from Netzsch. All measurements were performed under a nitrogen atmosphere (flow-rate: 20 mL min^{-1}) with Al_2O_3 crucibles. The heating rates are 10 K min^{-1}.

X-ray Powder Diffractometry: The X-ray powder diffraction patterns were acquired with a DMAX-2500 diffractometer by using Cu K_a radiation at ambient environment.

Supporting Information (see footnote on the first page of this article): DTA-TG figures of the title compounds and X-ray powder patterns of crystals **2** and **3**.

Acknowledgments

This work was supported by grants from the State Key Laboratory of Structure Chemistry, Fujian Institute of Research on the Structure of Matter, Chinese Academy of Sciences (CAS), the 973 Program (2006CB932900), the National Science Foundation of China (20333070, 90206040, 90406024, and 20673118), the Science Foundation of CAS, and Fujian Province (2006J0014, 2005HZ01–1, and 2004HZ01–1).

[1] L. Chen, X. T. Wu in *Inorganic Chemistry in Focus II* (Eds.: G. Meyer, D. Naumann, L. Weseman), Wiley; New York, **2005**, p. 207.

[2] X. T. Wu, Q. Huang, Q. M. Wang, T. L. Sheng, J. X. Lu in *Transition Metal Sulfur Chemistry: Biological and Industrial Significance* (Eds.: E. I. Stiefel, K. Matsumoto), ACS Symposium Series 653, American Chemical Society, Washington DC, **1996**, p. 282.

[3] M. Schaefer, D. Kurowski, A. Pfitzner, C. Na1ther, Z. Rejai, K. Mo1ller, N. Ziegler, W. Bensch, *Inorg. Chem.* **2006**, *45*, 3726.

[4] For examples, see: a) H. Yu, W. J. Zhang, X. T. Wu, T. L. Sheng, Q. M. Wang, P. Lin, *Angew. Chem. Int. Ed.* **1998**, *37*, 2520; b) Q. Huang, X. T. Wu, Q. M. Wang, T. L. Sheng, J. X. Lu, *Angew. Chem. Int. Ed. Engl.* **1996**, *35*, 868–869; c) Q. Huang, X. T. Wu, T. L. Sheng, Q. M. Wang, *Inorg. Chem.* **1995**, *34*, 4931–4932; d) Q. Huang, X. T. Wu, J. X. Lu, *Inorg. Chem.* **1996**, *35*, 7445–7447; e) Q. Huang, X. T. Wu, J. X. Lu, *Chem. Commun.* **1997**, 703; f) L. Chen, X. T. Wu, X. C. Gao, W. J. Zhang, P. Lin, *J. Chem. Soc., Dalton Trans.* **1999**, 4303–4307.

[5] R. Stähler, B.-D. Mosel, H. Eckert, W. Bensch, *Angew. Chem. Int. Ed.* **2002**, *41*, 4487.

[6] H.-O. Stephan, M. G. Kanatzidis, *J. Am. Chem. Soc.* **1996**, *118*, 12226.

[7] R. Stähler, W. Bensch, *Eur. J. Inorg. Chem.* **2001**, 3073.

[8] R. Stähler, W. Bensch, *J. Chem. Soc., Dalton Trans.* **2001**, 2518.

[9] H.-O. Stephan, M. G. Kanatzidis, *Inorg. Chem.* **1997**, *36*, 6050.

[10] R. Stähler, W. Bensch, *Z. Anorg. Allg. Chem.* **2002**, *628*, 1657.

[11] W. Bensch, C. Näther, R. Stähler, *Chem. Commun.* **2001**, 477.

[12] R. Stähler, C. Näther, W. Bensch, *Eur. J. Inorg. Chem.* **2001**, 1835.

[13] R. Stähler, C. Näther, W. Bensch, *J. Solid State Chem.* **2003**, *174*, 264.

[14] M. Schaefer, C. Näther, W. Bensch, *Solid State Sci.* **2003**, *5*, 1135.

[15] R. Kiebach, W. Bensch, R.-D. Hoffmann, R. Pöttgen, *Z. Anorg. Allg. Chem.* **2003**, *629*, 532.

[16] M. Schur, W. Bensch, *Z. Naturforsch., Teil B* **2002**, *57*, 1.

[17] W. Bensch, M. Schur, *Z. Naturforsch., Teil B* **1997**, *52*, 405.

[18] M. Schur, C. Näther, W. Bensch, *Z. Naturforsch., Teil B* **2001**, *56*, 79.

[19] L. Engelke, C. Näther, W. Bensch, *Eur. J. Inorg. Chem.* **2002**, 2936–2941.
[20] R. Kiebach, C. Näther, W. Bensch, *Z. Naturforsch., Teil B* **2004**, *59*, 1314–1319.
[21] X. Q. Wang, L. M. Liu, A. J. Jacobson, *J. Solid State Chem.* **2000**, *155*, 409–416.
[22] X. Q. Wang, F. Liebau, *J. Solid State Chem.* **1994**, *111*, 385–389.
[23] V. Spetzler, R. Kiebach, C. Näther, W. Bensch, *Z. Anorg. Allg. Chem.* **2004**, *630*, 2398–2404.
[24] P. Vaqueiro, D. P. Darlow, A. V. Powell, A. M. Chippindale, *Solid State Ionics* **2004**, *172*, 601–605.
[25] M. Schaefer, D. Kurowski, A. Pfitzner, C. Näther, W. Bensch, *Acta Crystallogr., Sect. E* **2004**, *60*, m183–m185.
[26] A. V. Powell, R. J. E. Lees, A. M. Chippindale, *Inorg. Chem.* **2006**, *45*, 4261–4267.
[27] A. Puls, M. Schaefer, C. Näther, W. Bensch, A. V. Powell, S. Boissière, A. M. Chippindale, *J. Solid State Chem.* **2005**, *178*, 1171–1181.
[28] R. Stähler, C. Näther, W. Bensch, *Acta Crystallogr., Sect. C* **2001**, *57*, 26–27.
[29] P. Vaqueiro, A. M. Chippindale, A. V. Powell, *Inorg. Chem.* **2004**, *43*, 7963–7965.
[30] D. X. Jia, Q. Y. Zhu, J. Dai, W. Lu, W. J. Guo, *Inorg. Chem.* **2005**, *44*, 819–821.
[31] D. X. Jia, Q. X. Zhao, Y. Zhang, J. Dai, J. L. Zuo, *Inorg. Chem.* **2005**, *44*, 8861–8867.
[32] R. Kiebach, F. Studt, C. Näther, W. Bensch, *Eur. J. Inorg. Chem.* **2004**, 2553–2556.
[33] D. X. Jia, Y. Zhang, J. Dai, Q. Y. Zhu, X. M. Gua, *J. Solid State Chem.* **2004**, *177*, 2477–2483.
[34] M. Schur, W. Bensch, *Acta Crystallogr., Sect. C* **2000**, *56*, 1107–1108.
[35] A. Puls, C. Näther, W. Bensch, *Acta Crystallogr., Sect. E* **2006**, *62*, m674–m676.
[36] L. Engelke, R. Stähler, M. Schur, C. Näther, W. Bensch, R. Pöttgen, M. H. Möller, *Z. Naturforsch., Teil B* **2004**, *59*, 869–876.
[37] A. Bondi, *J. Phys. Chem.* **1964**, *68*, 441.
[38] G. M. Sheldrick, *SHELXS-97*, University of Göttingen, Germany, **1997**.

Received: November 2, 2006
Published Online: February 28, 2007

